

A Model-Based Method for the Computation of Fingerprints' Orientation Field

Jie Zhou, *Member, IEEE*, and Jinwei Gu

Abstract—As a global feature of fingerprints, the orientation field is very important for automatic fingerprint recognition. Many algorithms have been proposed for orientation field estimation, but their results are unsatisfactory, especially for poor quality fingerprint images. In this paper, a model-based method for the computation of orientation field is proposed. First a combination model is established for the representation of the orientation field by considering its smoothness except for several singular points, in which a polynomial model is used to describe the orientation field globally and a point-charge model is taken to improve the accuracy locally at each singular point. When the coarse field is computed by using the gradient-based algorithm, a further result can be gained by using the model for a weighted approximation. Due to the global approximation, this model-based orientation field estimation algorithm has a robust performance on different fingerprint images. A further experiment shows that the performance of a whole fingerprint recognition system can be improved by applying this algorithm instead of previous orientation estimation methods.

Index Terms—Automatic fingerprint recognition, combination model, global approximation, orientation field, singular point.

I. INTRODUCTION

AMONG various biometric techniques, fingerprint recognition is regarded as most popular and reliable for automatic personal identification. During the last years it has received increasingly more attention [1]–[4]. Although the performance of fingerprint recognition systems is very good for applications on a small database, it is not satisfactory for large-scale applications [5].

A fingerprint is the pattern of ridges and valleys on the surface of a fingertip. In Fig. 1(a), a fingerprint is depicted. In this figure, the ridges are black and the valleys are white. Its orientation field, defined as the local orientation of the ridge-valley structures, is shown in Fig. 1(b). The minutiae, ridge endings and bifurcations, and the singular points, are also shown in Fig. 1(a). Singular points can be viewed as points where the orientation field is discontinuous. Fingerprints are usually partitioned into six main classes according to their macro-singularities, i.e., arch, tented arch, left loop, right loop, twin loop and whorl (see Fig. 2).

Manuscript received January 28, 2003; revised July 16, 2003. This work was supported by Natural Science Foundation of China under Grants 60205002 and 60332010, the Natural Science Foundation of Beijing under Grant 4042020, and the National 863 Hi-Tech Development Program of China under Grant 2001AA114190. The associate editor coordinating the review of this manuscript and approving it for publication was Dr. Thrasyvoulos N. Pappas.

The authors are with Department of Automation, Tsinghua University, Beijing 100084, China (e-mail: jzhou@tsinghua.edu.cn; gujinwei98@mails.tsinghua.edu.cn).

Digital Object Identifier 10.1109/TIP.2003.822608

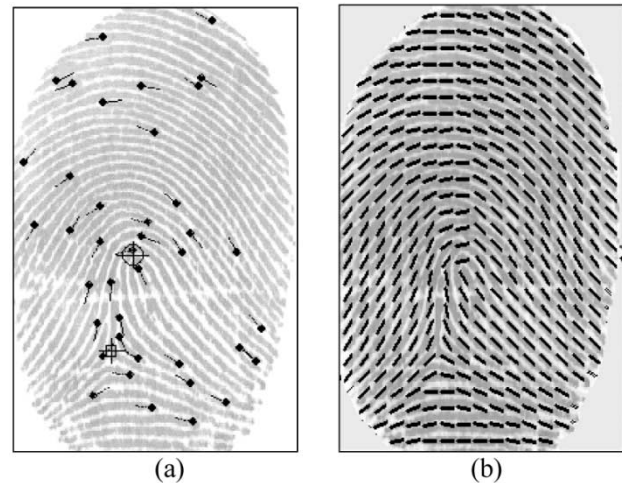


Fig. 1. Example of a fingerprint: (a) singular points and minutiae with its direction and (b) orientation field shown with unit vector.

Most classical fingerprint recognition algorithms [1], [2], [6], [7] take the minutiae and the singular points, including their coordinates and direction, as the distinctive features to represent the fingerprint in the matching process. Minutiae extraction mainly includes the below steps: orientation field estimation, ridge extraction or enhancement, ridge thinning and minutiae extraction. Then the minutiae feature is compared with the minutiae template; if the matching score exceed a predefined threshold, these two fingerprints can be regarded as belonging to a same finger. See Fig. 3 for the flowchart of conventional fingerprint recognition algorithms. As shown above, the estimation of orientation field is usually a basic step for a whole recognition system. So, an algorithm to estimate orientation field accurately and robustly is desired. Furthermore, it is also important for fingerprint classification and matching [9]–[11].

Many algorithms have been proposed for orientation field estimation, which include gradient-based approaches [6]–[9], filter-bank based approaches [10], [11], methods based on high-frequency power in 3-D space [12], 2-D spectral estimation methods [13] and micro-patterns as binary gradients [14]. Among these methods, the former two approaches are used popularly. The filter-bank based approaches are more resistant to noise (including smudges, breaks and creases, etc.) than the gradient-based, but they do not provide as much accuracy as the gradient-based approaches because of the limited number of the filters. Furthermore, it is computationally expensive because the comparison of all filters' output needs to be done.

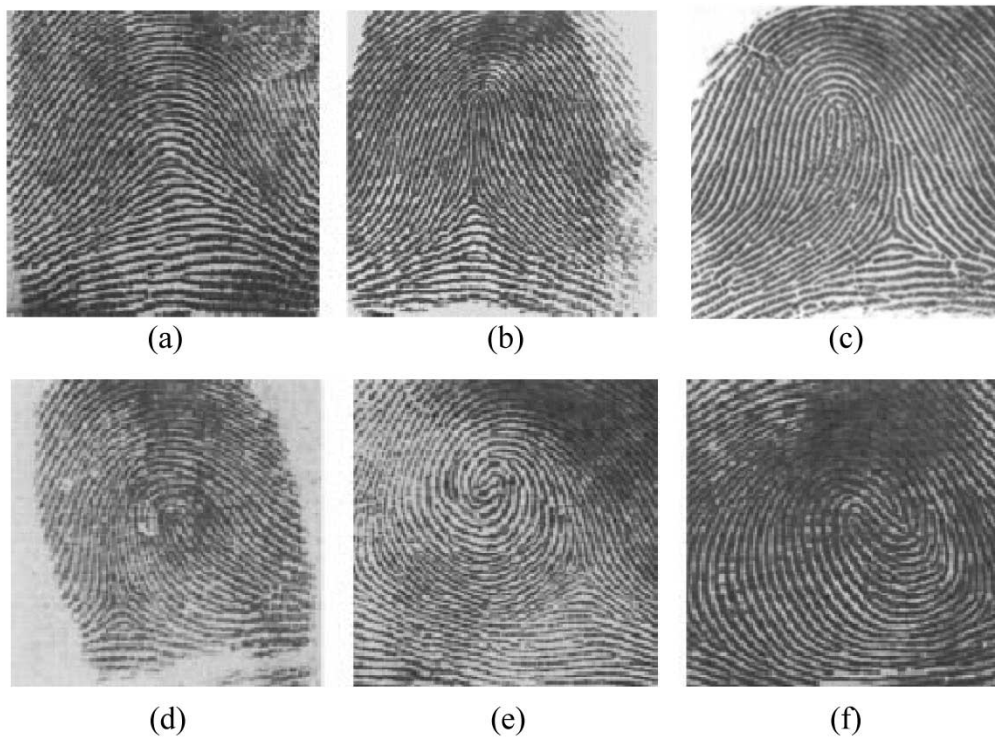


Fig. 2. One fingerprint for each of the six main classes: (a) arch, (b) tented arch, (c) left loop, (d) right loop, (e) whorl, and (f) twin loop.

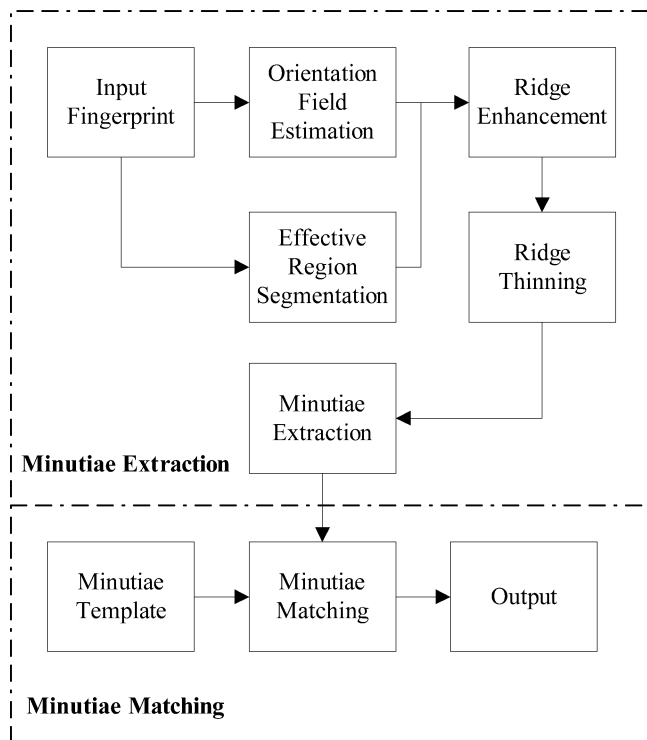


Fig. 3. Flowchart of the conventional fingerprint recognition systems.

Contrastively, the gradient-based approaches can provide continuous value but lack in robustness to the noise. In order to eliminate the affection of noise, the authors of [6], [7] proposed a hierarchical scheme for the implement for gradient-based algorithm. The orientation of each point is compared with its neighborhood and if they are not consistent, the local orienta-

tions around this region are re-estimated in a lower resolution level until the consistency is below a certain level. In [8], the authors utilized Principal Component Analysis for orientation extraction of a small region after the gradient computation. It is proven that this method provides exactly the same results with the averaged square gradient algorithm. Because the steps are taken locally in these methods, the improvement is rather limited (see [6]–[8] for details). Additionally, a diffusion-based orientation smoothing method was proposed in [15], in which a definition of continuum was introduced and based on it, an iterative algorithm of discrete orientation diffusion was established. It can be used to extract singular points in the fingerprint images, but how to apply it into robust orientation estimation for fingerprint recognition was not studied. Also, it is not suitable for on-line processing due to its iteration.

In this paper, we will propose a novel algorithm for orientation field estimation. Since the orientation field is rather smooth except for several singular points, we can establish a polynomial model to globally represent the orientation field and use a point-charge model to improve the accuracy locally at each singular point. When the coarse field is computed by using conventional gradient-based algorithm, the model is utilized to compute the finer field. Since the noise can be discarded in the approximation step, the final estimated result of orientation field has a robust performance while preserving the accuracy.

The paper is organized as follows. In Section II, the combination model of the orientation field is proposed. The algorithm for computing the orientation field using the above model is given in Section III. Experimental results of orientation estimation evaluation and application evaluation are presented in Section IV. We finish with conclusions and discussion in Section V.

II. COMBINATION MODEL OF ORIENTATION FIELD

Sherlock and Monro [16] proposed a so-called zero-pole model for orientation field based on singular points, which takes the core as zero and the delta as a pole in the complex plane. The influence of a core z_c , is $1/2 \arg(z - z_c)$ for the point z , and that of a delta z_d is $-1/2 \arg(z - z_d)$. The orientation at z is the sum of the influence of all cores and deltas. It is simple but inaccurate because many fingerprints that have the same singular points may yet differ in detail. Vizcaya and Gerhardt [17] had made an improvement using a piecewise linear approximation model around singular points to adjust the zero and pole's behavior. First, the neighborhood of each singular point is uniformly divided into eight regions and the influence of the singular point is assumed to change linearly in each region. An optimization implemented by gradient-descend is then performed to get a piecewise linear function. These two models cannot deal with fingerprint without singular point such as the plain arch classified by Henry [18]. Furthermore, since they do not consider the distance from singular points and the influence of a singular point is the same as any point on the same central line, whether near or far from the singular point, serious error will be caused in the modeling of the regions far from singular points. As a result, these two models cannot be used for accurate approximation to real fingerprint's orientation field.

Here we propose a combination model for the orientation matrix. Since the orientation of fingerprints is quite smooth and continuous except at singular points, we apply a polynomial model to approximate the global orientation field. At each singular point, a point-charge model similar to the zero-pole model is used to describe the local region. Then, these two models are combined smoothly together through a weight function.

From Fig. 1(b), we can see that the orientation pattern of a fingerprint is quite smooth and continuous except near the singular points. That means we can apply a simple and smooth function to approximate it globally. Since the value of a fingerprints' orientation is defined within $[0, \pi)$, therefore it seems that this representation has an intrinsic discontinuity (in fact, the orientation, 0, is the same as the orientation, π , in ridge pattern). So we cannot model the orientation field directly. A solution to this problem is to map the orientation field to a continuous complex function [19], [20]. Denoting $\theta(x, y)$ and $U(x, y)$ as the orientation field and the transformed function, respectively, the mapping can be defined as

$$U = RE + i IM = \cos 2\theta + i \sin 2\theta \quad (1)$$

where RE and IM denote respectively the real part and imaginary part of the complex function, $U(x, y)$. Obviously, $RE(x, y)$ and $IM(x, y)$ are continuous with x, y in those regions. The above mapping is a one-to-one transformation and $\theta(x, y)$ can be easily reconstructed from the values of $RE(x, y)$ and $IM(x, y)$.

To globally represent $RE(x, y)$ and $IM(x, y)$, two bivariate polynomial models are established, which are denoted by PR , PI respectively. These two polynomials can be formulated as

$$PR(x, y) = (1 \quad x \quad \cdots \quad x^n) \cdot P_1 \cdot \begin{pmatrix} 1 \\ y \\ \vdots \\ y^n \end{pmatrix} \quad (2)$$

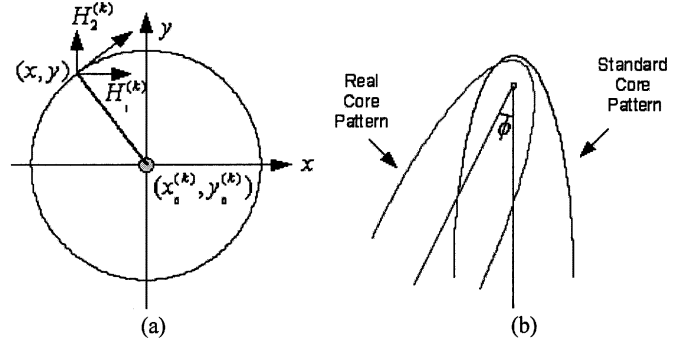


Fig. 4. An illumination for the point-charge model: (a) influence vector around a standard core and (b) real ridge pattern near a core with a rotation angle, ϕ .

and

$$PI(x, y) = (1 \quad x \quad \cdots \quad x^n) \cdot P_2 \cdot \begin{pmatrix} 1 \\ y \\ \vdots \\ y^n \end{pmatrix} \quad (3)$$

where n is the polynomials' order and the matrices, $P_i \in \mathbb{R}^{n \times n}$, $\forall i = 1, 2$.

Near the singular points, the orientation is no longer smooth, so it is difficult to model with a polynomial function. A model named 'point-charge' (PC) is added at each singular point. Compared with the model provided in [16], the point-charge model uses different quantities of electricity to describe the neighborhood of each singular point instead of the same influence at all singular points. And for a certain singular point, its influence at the point, (x, y) , varies with the distance between the point and the singular point. Fig. 4(a) shows the unit influence vector (tangent vector) caused by a standard core. Its electric flux lines are clockwise along the concentric circle. The influence of a standard (vertical) core at the point, (x, y) , is defined as

$$PC_{Core} = H_1 + iH_2 = \begin{cases} \frac{y-y_0}{r}Q - i\frac{x-x_0}{r}Q, & r \leq R, \\ 0, & r > R \end{cases} \quad (4)$$

where (x_0, y_0) is this core's position, Q is the quantity of electricity, R denotes the radius of its effective region, and $r = \sqrt{(x-x_0)^2 + (y-y_0)^2}$. The radius of a standard delta is

$$PC_{Delta} = H_1 + iH_2 = \begin{cases} -\frac{y-y_0}{r}Q - i\frac{x-x_0}{r}Q, & r \leq R, \\ 0, & r > R. \end{cases} \quad (5)$$

In a real fingerprint image, the ridge pattern at the singular points may have a rotation angle compared with the standard one. If the clockwise rotation angle from standard position is ϕ ($\phi \in (-\pi, \pi]$, see Fig. 4(b)), a transformation can be made as

$$\begin{pmatrix} x' \\ y' \end{pmatrix} = \begin{pmatrix} x_0 \\ y_0 \end{pmatrix} + \begin{pmatrix} \cos \phi & \sin \phi \\ -\sin \phi & \cos \phi \end{pmatrix} \cdot \begin{pmatrix} x - x_0 \\ y - y_0 \end{pmatrix}. \quad (6)$$

Then, the point-charge model can be modified by taking x' and y' instead of x and y , for cores in (4) and deltas in (5), respectively.

To combine the polynomial model, (PR, PI) , with the point-charge model smoothly, a weight function can be used. For the

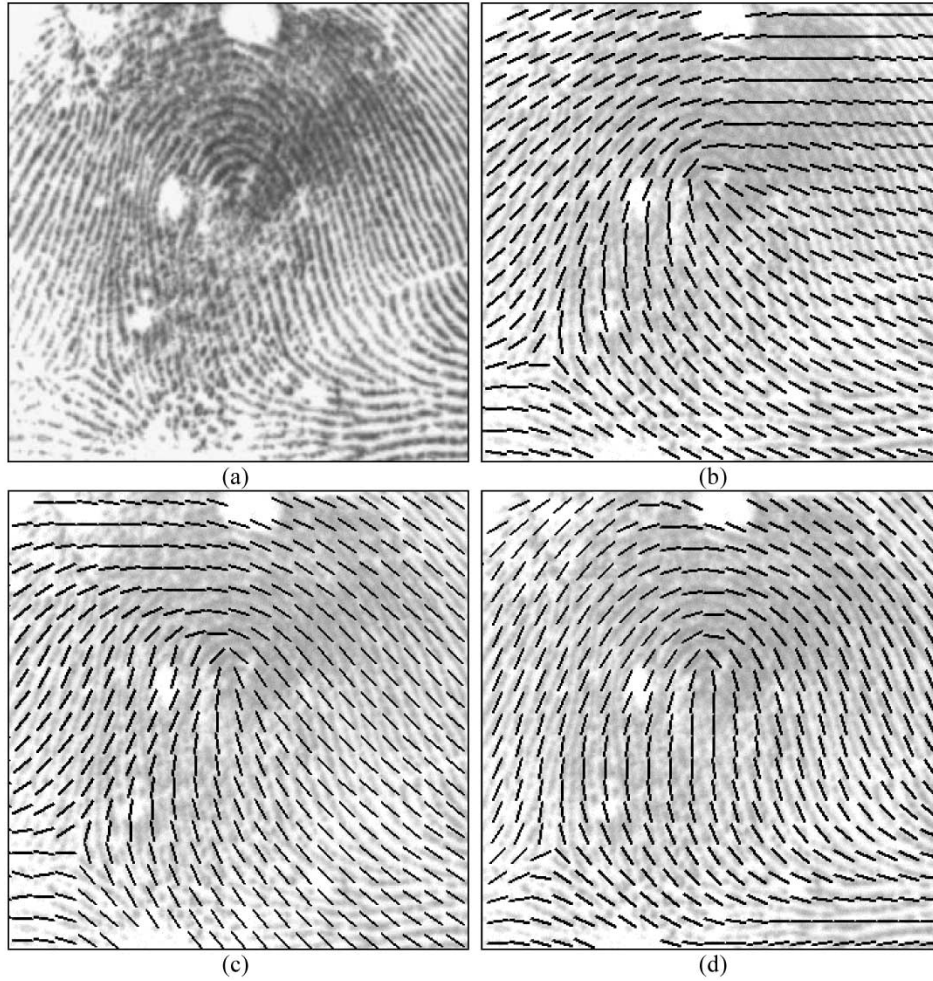


Fig. 5. Comparison of three models: (a) original fingerprint, (b) the reconstructed orientation field using the zero-pole model [16], (c) the piecewise linear model [17], and (d) the combination model proposed in this paper.

point-charge model, the weighting factor at the point, (x, y) , is defined as

$$\alpha_{PC}^{(k)}(x, y) = 1 - \frac{r^{(k)}(x, y)}{R^{(k)}} \quad (7)$$

where $(x_0^{(k)}, y_0^{(k)})$ is the coordinate of the k -th singular point, $R^{(k)}$ is the radius of the effective region, and $r^{(k)}(x, y)$ is set as $\min(\sqrt{(x - x_0^{(k)})^2 + (y - y_0^{(k)})^2}, R^{(k)})$. For the polynomial model, the weighting factor at the point, (x, y) , is:

$$\alpha_{PM}(x, y) = \max \left\{ 1 - \sum_{k=1}^K \alpha_{PC}^{(k)}, 0 \right\} \quad (8)$$

where K is the number of singular points. The weight function guarantees that for each point, its orientation follows the polynomial model if it is far from the singular points and follows the point-charge model if it is near one of the singular points.

Then, the combination model for the whole fingerprint's orientation field can be formulated as

$$\begin{pmatrix} RE(x, y) \\ IM(x, y) \end{pmatrix} = \alpha_{PM} \cdot \begin{pmatrix} PR \\ PI \end{pmatrix} + \sum_{k=1}^K \alpha_{PC}^{(k)} \cdot \begin{pmatrix} H_1^{(k)} \\ H_2^{(k)} \end{pmatrix} \quad (9)$$

with the constrain of

$$RE^2(x, y) + IM^2(x, y) = 1 \quad (10)$$

where PR and PI are respectively the real and imaginary part of the polynomial model, and $H_1^{(k)}$ and $H_2^{(k)}$ are respectively the real and imaginary part of the point-charge model for the k -th singular point. Obviously, the combination model is continuous with x and y . The coefficient matrices of the two polynomials, PR and PI , and the electrical qualities, $\{Q_1, Q_2, \dots, Q_K\}$, of the singular points will define the combination model.

Compared with the models proposed in [16] and [17], the advantages of our combination model are as below: 1) it can accurately represent the orientation field in regions either near or far from singular points; and 2) it is also suitable for plain arch fingerprints which have no singular points. An example is given in Fig. 5, in which (a) is the original fingerprint, (b) (c) and (d) are the reconstructed orientation field using the zero-pole model [16], piecewise linear model [17] and the combination model, respectively. All of them use the same algorithm for singular point extraction. It shows that only the combination model can describe the orientation of the whole fingerprint image smoothly and precisely, whether the region is near or far from the singular

points. As a result, it can be further utilized for the aim of this paper, i.e., the computation of finer orientation field.

III. MODEL-BASED ORIENTATION FIELD ESTIMATION

Based on the combination model in Section II, a novel method of orientation field estimation can be proposed. Its steps are described as below.

A. Computation of Coarse Orientation Field

In order to get an accurate representation of orientation field, we adopt a gradient-based approach for the computation of coarse orientation field in our work.

It has been demonstrated that for a strongly oriented intensity pattern along one direction, the power spectrum of such a pattern clusters along a line through the origin in Fourier transformation domain and the direction of the line is perpendicular to the dominant spatial orientation. In stead of the actual computation in the Fourier transformation domain, the orientation map, $O(x, y)$, and anisotropic strength map, $W(x, y)$, can be calculated directly by

$$O(x, y) = \frac{1}{2} \tan^{-1} \frac{\sum_{\Gamma} 2G_x G_y}{\sum_{\Gamma} (G_x^2 - G_y^2)} + \frac{\pi}{2} \quad (11)$$

and

$$W(x, y) = \frac{(\sum_{\Gamma} (G_x^2 - G_y^2))^2 + 4(\sum_{\Gamma} G_x G_y)^2}{(\sum_{\Gamma} (G_x^2 + G_y^2))^2} \quad (12)$$

where Γ is a small neighboring region of the point, (x, y) , (G_x, G_y) is the gradient vector at (x, y) , \tan^{-1} is a 4-quadrant arctangent function and the output of \tan^{-1} is within $(-\pi, \pi)$. Note that Γ is a small neighborhood of pixel (x, y) , whose size is related with the size of the object (the width of ridge in our work). The value of anisotropic strength, W , is between 0 and 1 (close to 1 for a strongly oriented pattern, and 0 for isotropic regions), which can also be seen as the reliability of the orientation computed by using (11) [21]–[24].

B. Extraction of Singular Points

To implement our algorithm, we also need to identify the position and type of singular points. Many approaches have been proposed for singular point extraction [3], [4], [8], [9], [14]–[16]. Among them, the algorithms based on the Poincare index are used popularly.

Following a counterclockwise closed contour around a core in the orientation field and adding the differences between the subsequent angles results in a cumulative change in the orientation of π and carrying out this procedure around a delta results in $-\pi$. However the cumulative orientation change will be zero when the procedure is applied to nonsingular points. Based on the above rules, a small two-dimensional filter is developed to extract all singular points, including some false singular points caused by irregular orientation field [8]. Then some steps are further taken to verify the detected point and tell whether it is a core, a delta or a false singular point.

C. Model-Based Approximation

The two bivariate polynomials can be computed by using the Weighted Least Square (WLS) algorithm [25]. The coefficients of the polynomial are obtained by minimizing the weighted square error between the polynomial and the values of $RE(x, y)$ and $IM(x, y)$ computed from the coarse orientation field. As pointed above, the reliability, $W(x, y)$, can indicate how well the orientation fits the real ridge. The higher the reliability is, the more influence the point should have. Then $W(x, y)$ can be used in the weighting factor at the point, (x, y) . As a result, it can efficiently decrease the influence of inaccurate orientation estimation.

As we know, the higher order polynomial can provide a better approximation, but at the same time it will results in less generalization and much higher cost of computation. In our study, we choose 4-order ($n = 4$) polynomials for the global approximation. The experimental results showed that they performed well enough for most real fingerprints, while preserving a small cost for storage and computation.

The coefficients of the point-charge model at singular points can be obtained in two steps. First, two parameters are estimated for each singular point: the rotation angle, ϕ , and the effective radius, R . Second, charges of singular points are estimated by optimization.

Since the average orientation near the singular point can be inferred from the result of polynomial approximation, the rotation angle, ϕ , which can be regarded as the cross angle between the vertical line and the average orientation of the ridge pattern around the singular point, can be easily computed. For cores, we can further tell whether it is upward or downward by matching the core with an upward core and a downward core template, which are generated from the standard point-charge model. For the convenience of computation, the value of R can be set in advanced. In our experiments, R is chosen as 80 pixels for each core regardless of the difference of fingerprint images. When dealing with deltas, it is set as 40 pixels for all fingerprint images.

After that, we need to estimate the charges for singular points. Since our purpose is to minimize the approximation error, the objective function for the singular points can be represented as

$$\min J = \sum_{\Omega} \left([RE(x, y) - \cos 2O]^2 + [IM(x, y) - \sin 2O]^2 \right) \quad (13)$$

where O is the original orientation field and Ω is the effective region for the point-charge model. For each singular point, its effective region is a small circle with radius R . Ω is the union set of all these small circles. The variables in the above optimization problem are the charges of singular points, $\{Q_1, Q_2, \dots, Q_K\}$. They can be computed by solving the following equations as

$$\frac{\partial J}{\partial Q_k} = 0, \quad k = 1, 2, \dots, K. \quad (14)$$

Then, all the coefficients of the model have been computed. That means we can reconstruct the orientation field using these coefficients. Note that the constraint of (10) need not be used in the above steps because the values of $RE(x, y)$ and $IM(x, y)$ from the coarse orientation field have satisfied it. The approximation results can surely keep a similar property.

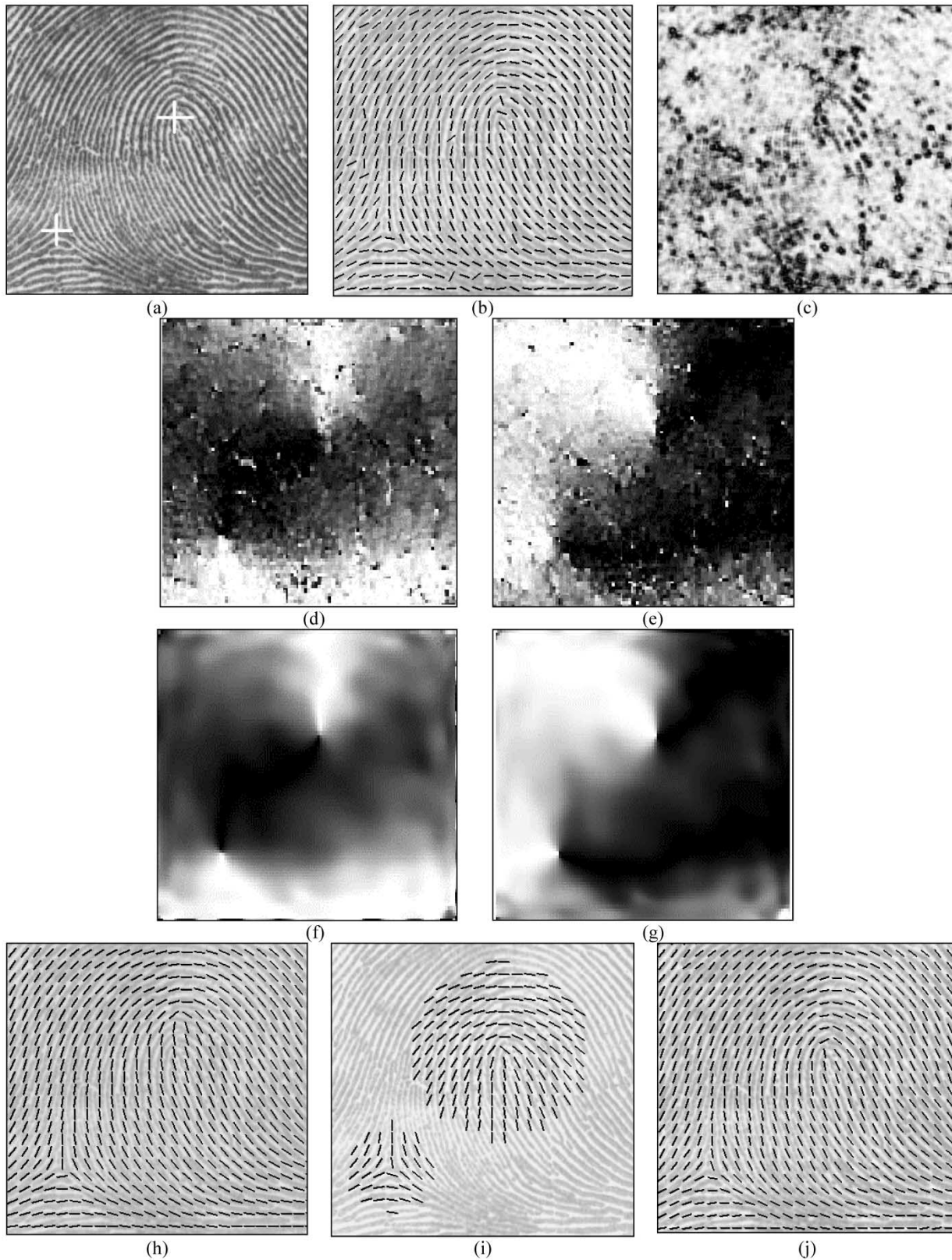


Fig. 6. The results of each step in our implement scheme: (a) original fingerprint with singular points marked; (b) the coarse orientation field, O ; (c) the reliability map, W ; (d) and (e) are $\cos(2O)$ and $\sin(2O)$, i.e. the transformed images of the coarse orientation field, O ; (f) and (g) are the approximation results from (d) and (e), respectively, i.e., the transformed images of the reconstructed orientation field; (h), (i) and (j) are the reconstructed orientation field by using the polynomial model, point charge model and the combination model, respectively.

In Fig. 6, the results of each step in our implement scheme are listed. (a) is the original fingerprint with singular points marked; (b) is the coarse orientation field, O , computed by using gra-

dent-based method; (c) is the reliability map, W ; (d) and (e) are the transformed images, $\cos(2O)$ and $\sin(2O)$, of the coarse orientation field, O ; (f) and (g) are the approximation results from

TABLE I

ESTIMATED VALUES OF THE COEFFICIENTS MATRIX, P_1 , FOR THE POLYNOMIAL MODEL (CORRESPONDING TO FIG. 6), WHERE THE ORIGIN OF THE COORDINATES IS CHOSEN AS THE IMAGE'S CENTER, x -AXIS IS FROM LEFT TO RIGHT HORIZONTALLY AND y -AXIS IS FROM DOWN TO UP VERTICALLY

	1	x	x^2	x^3	x^4
1	-7.8438e-001	1.9917e-003	2.0761e-006	-3.0891e-008	6.9663e-011
y	4.4940e-003	-6.7147e-007	-4.0080e-007	-1.0381e-010	4.9800e-012
y^2	8.2981e-005	4.7903e-008	-1.4876e-009	-3.6954e-013	1.2433e-014
y^3	-1.3853e-007	1.0910e-010	7.7127e-012	3.3846e-016	-8.4374e-017
y^4	-1.1518e-009	-2.8448e-012	3.6522e-014	2.5511e-017	-4.3809e-019

TABLE II

ESTIMATED VALUES OF THE COEFFICIENTS MATRIX, P_2 , FOR THE POLYNOMIAL MODEL (CORRESPONDING TO FIG. 6), WHERE THE ORIGIN OF THE COORDINATES IS CHOSEN AS THE IMAGE'S CENTER, x -AXIS IS FROM LEFT TO RIGHT HORIZONTALLY AND y -AXIS IS FROM DOWN TO UP VERTICALLY

	1	x	x^2	x^3	x^4
1	-2.6544e-001	-6.0876e-003	4.6536e-006	5.0258e-008	-2.3940e-011
y	9.0604e-003	-3.8196e-005	-4.8907e-007	9.4291e-010	5.7193e-012
y^2	-4.1217e-006	-4.6452e-008	5.2624e-010	-2.6768e-013	-4.1850e-015
y^3	-2.1019e-007	4.9850e-010	9.2636e-012	-1.8273e-014	-8.7261e-017
y^4	3.1875e-010	2.0254e-012	-1.6866e-014	1.6578e-017	1.6555e-019

(d) and (e), respectively, i.e. the transformed images of the reconstructed orientation field; (h), (i) and (j) are the reconstructed orientation fields by using the polynomial model, point-charge model and the combination model, respectively. In Table I and Table II, the estimated values of the coefficient matrices, P_1 and P_2 (in (2), (3)), for the polynomial model are provided, where the origin of the coordinates is chosen as the image's center, x -axis is from left to right horizontally and y -axis is from down to up vertically. The charges of the core point and delta point are 4.8138e-001 and 9.3928e-001, respectively. The rotation angles of the core point and delta point are -15.4 degree and -2.4 degree, respectively. Comparing (h) and (j), we can find that the estimated orientation field by only using polynomial model is rather accurate except for a small neighborhood of the core point. It shows that the orientation field of a fingerprint can be approximated globally by only using the polynomial model, guaranteeing the performance of our model-based method in cases of displaced, false or missing singular points while dealing with poor-quality fingerprint images.

IV. EXPERIMENTAL RESULTS

Two experiments are carried to test the performance of our algorithm. First, we apply our algorithm to some fingerprint images and evaluate the accuracy and robustness of orientation estimation. The second experiment is an application evaluation of orientation field estimation in terms of a fingerprint recognition application.

A. Orientation Estimation Evaluation

This experiment is carried on 480 fingerprint images from 3 sets. Set 1 contains a sample set of 40 rolled and inked fingerprints from NIST Special Database 14 [26]; Set 2 includes 320 fingerprint images from FVC2000's sample database [27], which contains 4 subset collected with different sensor/technologies; Set 3 includes 120 fingerprint images selected from THU database of our own lab, which are captured with live-scanners. These fingerprint images have different sizes and vary in different qualities. In them, more than 40% of these images are suffering the affection from large creases, scars and smudges in the ridges or dryness and blurs of the fingers. In Fig. 7, some tested fingerprint images are listed. These fingerprints are from different parts of the database. Among them there are various fingerprint types: plain arch, tented arch, right loop, left loop, whorl, twin loop and accidental type.

Three algorithms for orientation field estimation are evaluated on the database: the hierarchical gradient-based algorithm [6], [7] (in which the threshold of consistency level is chosen as $\pi/6$), the filter bank-based algorithm [10] and the model-based algorithm. In global approximation of our algorithm, 4-order bivariate polynomials are employed. In the algorithm based on Gabor filter bank, totally 64 filters are used in order to get an accurate output. Consequently, it is very expensive of computation. When implemented with C on a AMD 2200 Hz PC computer, the average computational time for an image sized 512×320 is about 1.0 seconds, 10 seconds and 0.8 second, respectively, by using the hierarchical gradient-based algorithm, filter bank-based algorithm and the model-based algorithm (including singular points extraction). That is to say, the ratio between the computational cost is about 1.2: 12.5: 1 for these three algorithms. Compared with the other two algorithms especially for the filter bank-based algorithm, the model-based algorithm has an evident advantage of low computational cost.

Since no ground truth exists for the orientation field of fingerprints, objective error measurement cannot be easily constructed. Therefore it is difficult to evaluate the quality of estimated orientation field quantitatively. Alternatively, the quality of the estimation has to be assessed by means of manual inspection. From observation, it can be concluded that the performance of our algorithm is satisfactory. Compared with the other two algorithms, our algorithm is more robust to different noise while preserving the accuracy.

Some of the results of our algorithm are presented in Fig. 8. The reconstructed orientation fields are shown as unit vectors upon the original fingerprint, which correspond to the images listed in Fig. 7. As shown, the results are rather accurate and robust for these fingerprints.

Fig. 9 and Fig. 10 give two examples for comparison, where (a) is the original fingerprint, (b) is the orientation field marked manually, (c) is the coarse orientation field estimated by using (11), (d) is the orientation estimated by using the hierarchical gradient-based method [6], [7], (e) the orientation field estimated by Gabor filter-bank (64 filters) method [10], and (f) are the estimated orientation field by using our model-based algorithm. The computed orientation fields are also shown as unit vectors upon the original fingerprint. The results show that:



Fig. 7. Some fingerprint images used in our experiments: (a) plain arch, (b) left loop, (c) right loop, (d) tented arch, (e) whorl, (f) whorl, (g) twin loop, and (h) accidental class.

the coarse orientation computed directly from gradient-based algorithm (in (11)) is easily affected by the noise; although the performances of hierarchical gradient-based algorithm is better than directly using gradient-based algorithm, it still

lacks in accuracy against strong noise; Gabor filter-bank based algorithm also produces wrong results in some regions, such as in the bottom-right of Fig. 9(e) and the middle-top of Fig. 10(e); contrastively, our model-based algorithm, though based on the

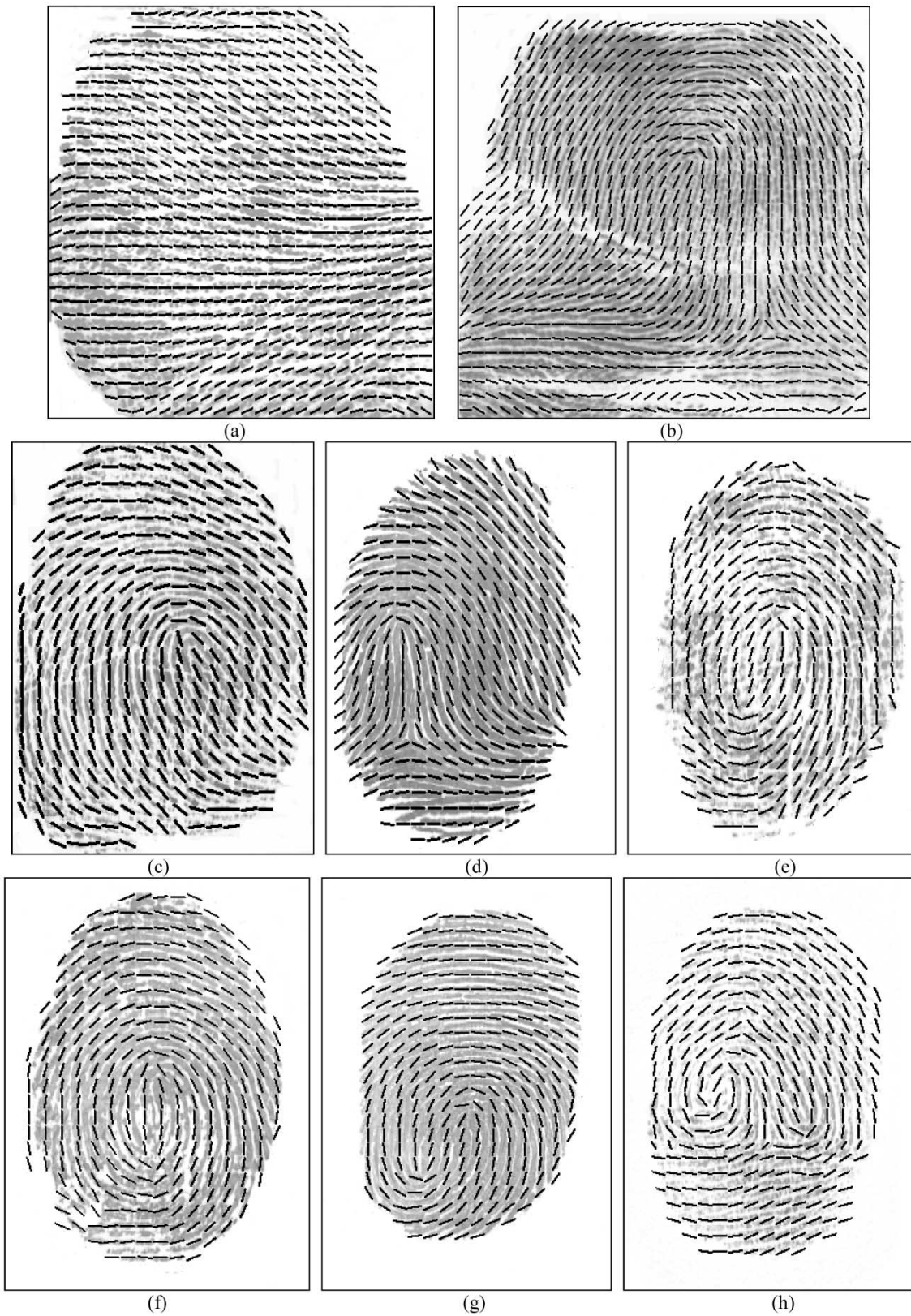


Fig. 8. Some results of our algorithm, in which the estimated orientation field is shown with unit vectors upon the original fingerprints (corresponding to the images in Fig. 7).

coarse orientation field, can reconstruct the orientation field most smoothly and accurately.

In our experiments, the model-based algorithm has a satisfying performance for most fingerprint images. But for a few very poor-

quality fingerprints, if the original orientation field is too unreliable, or if one cannot extract the singular points correctly at all, the approximation performance of the combination model will be bad. In Fig. 11, an example is given, in which (a) is the input

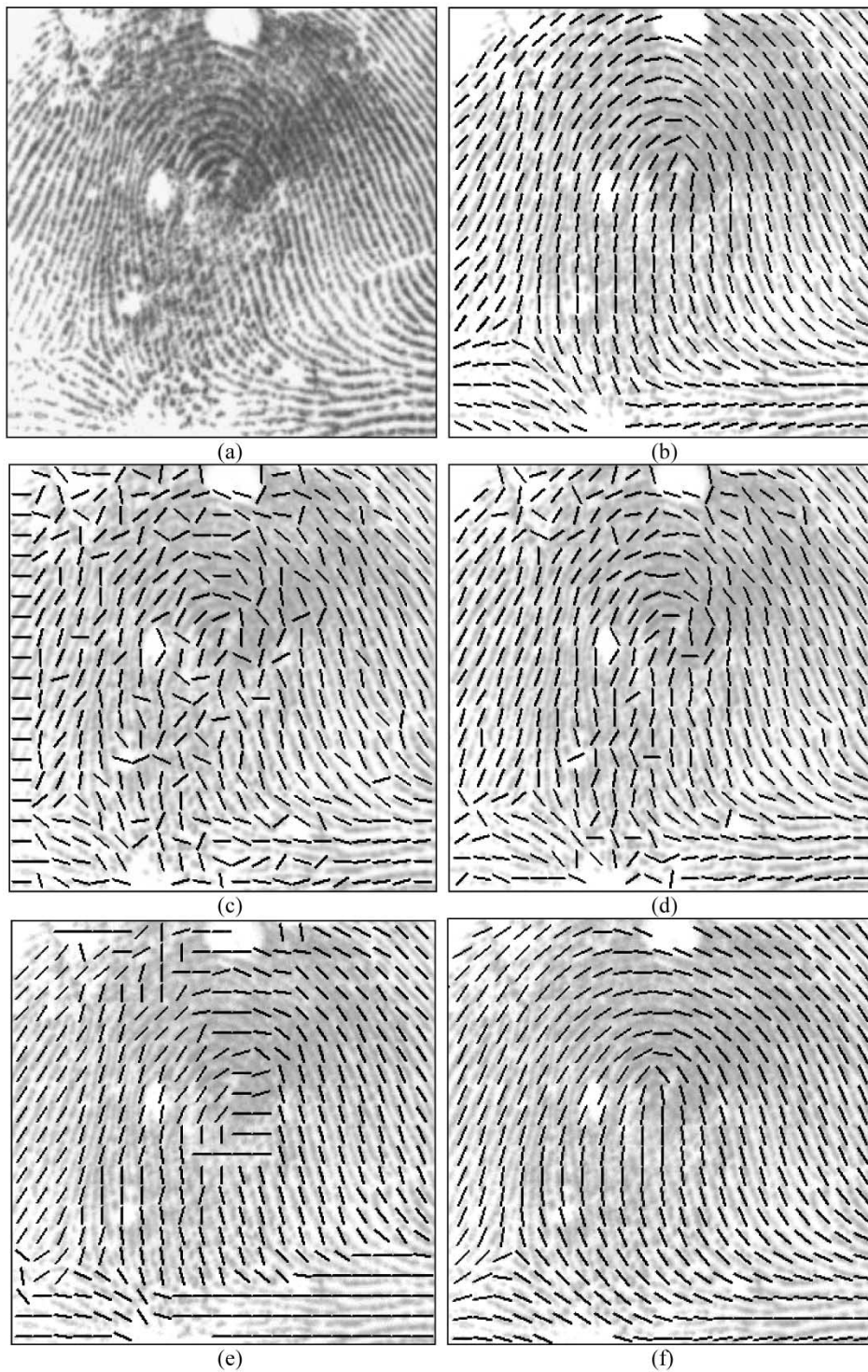


Fig. 9. Comparative result I: (a) original fingerprint from Set 1; (b) is the orientation field marked manually, (c) is the coarse orientation field estimated by using (11), (d) is the orientation estimated by using the hierarchical gradient-based method [6], [7], (e) the orientation field estimated by Gabor filter-bank (64 filters) method [10], and (f) are the estimated orientation field by using our model-based algorithm.

fingerprint; (b) is the original orientation field obtained by conventional gradient-based method; and (c) is the orientation fields reconstructed by our combination model. Since (a) is too noisy in the right-bottom part, there is no reliable orientation information in (b). Consequently, the orientation field reconstructed by our model will fail in the right-bottom part, as in (c).

Since the combination model for the fingerprint's orientation field relies on the detected singular points, the performance of

the model-based algorithm will also be influenced by the results of singular points (cores and deltas) detection. In fact, it is quite difficult to reliably estimate the singular points in very poor quality fingerprint images. A false singular point may be detected in a very poor-quality region; from the other hand, the real singular points may also be missed if they exist in a very poor-quality region. Comparatively, displaced singular points (whose detected position is different with the real position) may

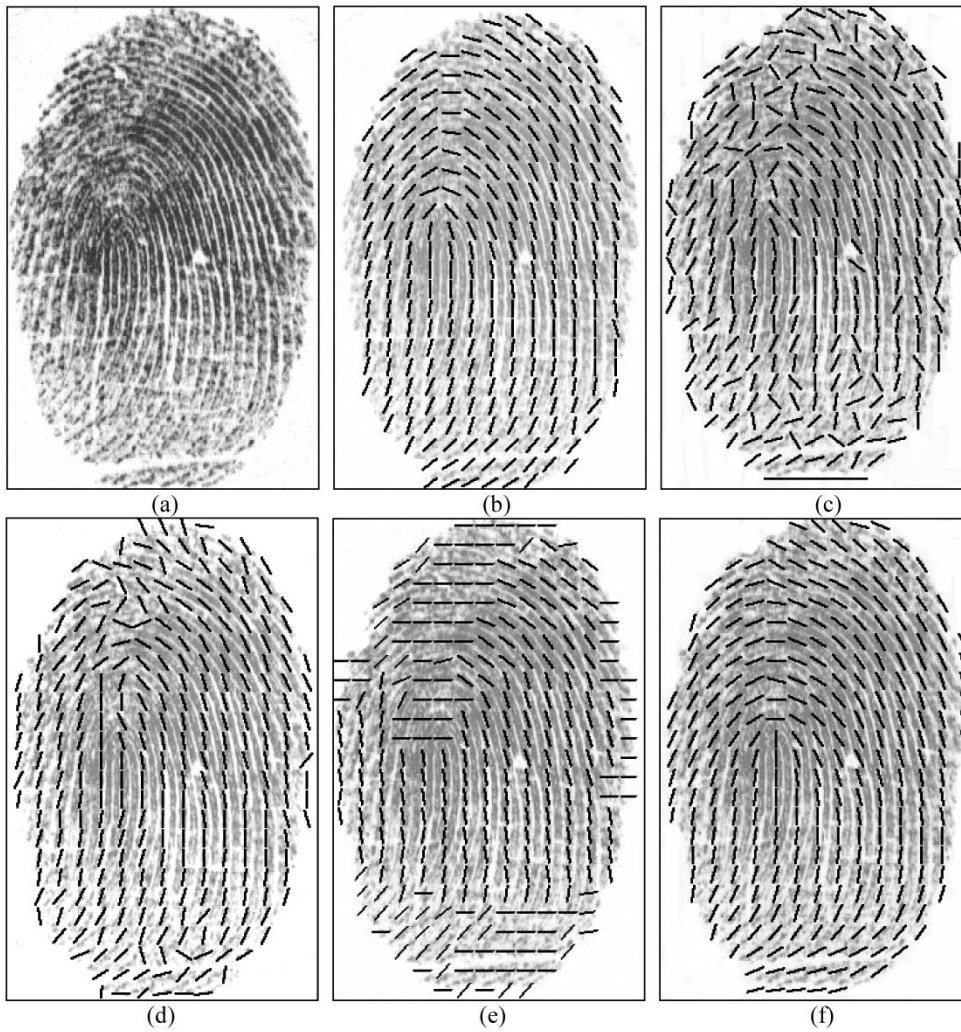


Fig. 10. Comparative result II: (a) original fingerprint from Set 3; (b) is the orientation field marked manually, (c) is the coarse orientation field, (d) is the orientation estimated by using the hierarchical gradient-based method [6], [7], (e) the orientation field estimated by Gabor filter-bank (64 filters) method [10], and (f) are the estimated orientation field by using our model-based algorithm.

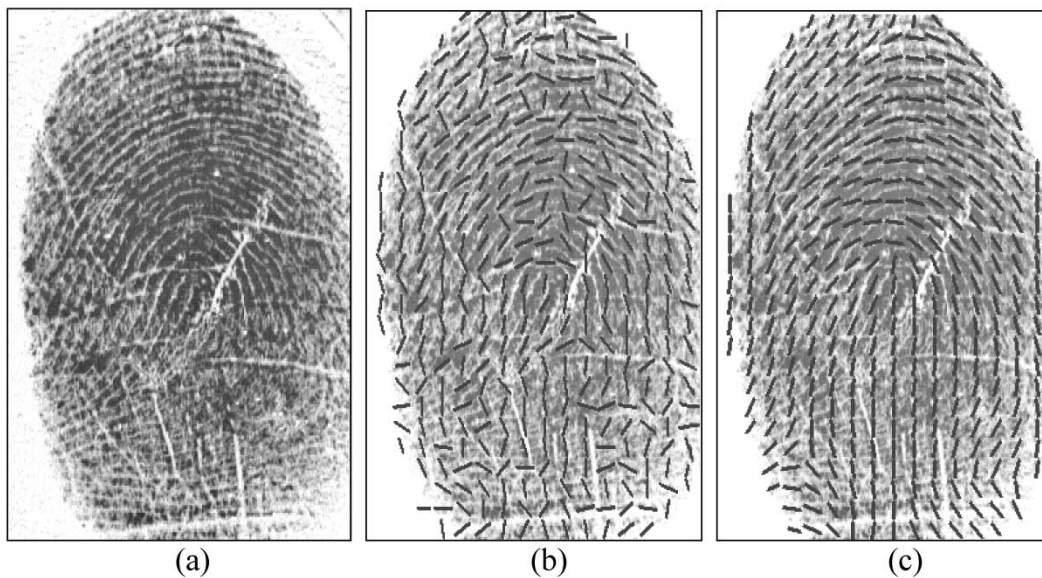


Fig. 11. A failure example of the model-based algorithm: (a) is the input fingerprint; (b) is the coarse orientation field obtained by gradient-based method; and (c) is the orientation fields reconstructed by the model-based method. In (a), the original image is too noisy in the right-bottom part and there is no reliable orientation information in that part of (b). Consequently, the orientation field reconstructed by the model-based method will fail in that region.

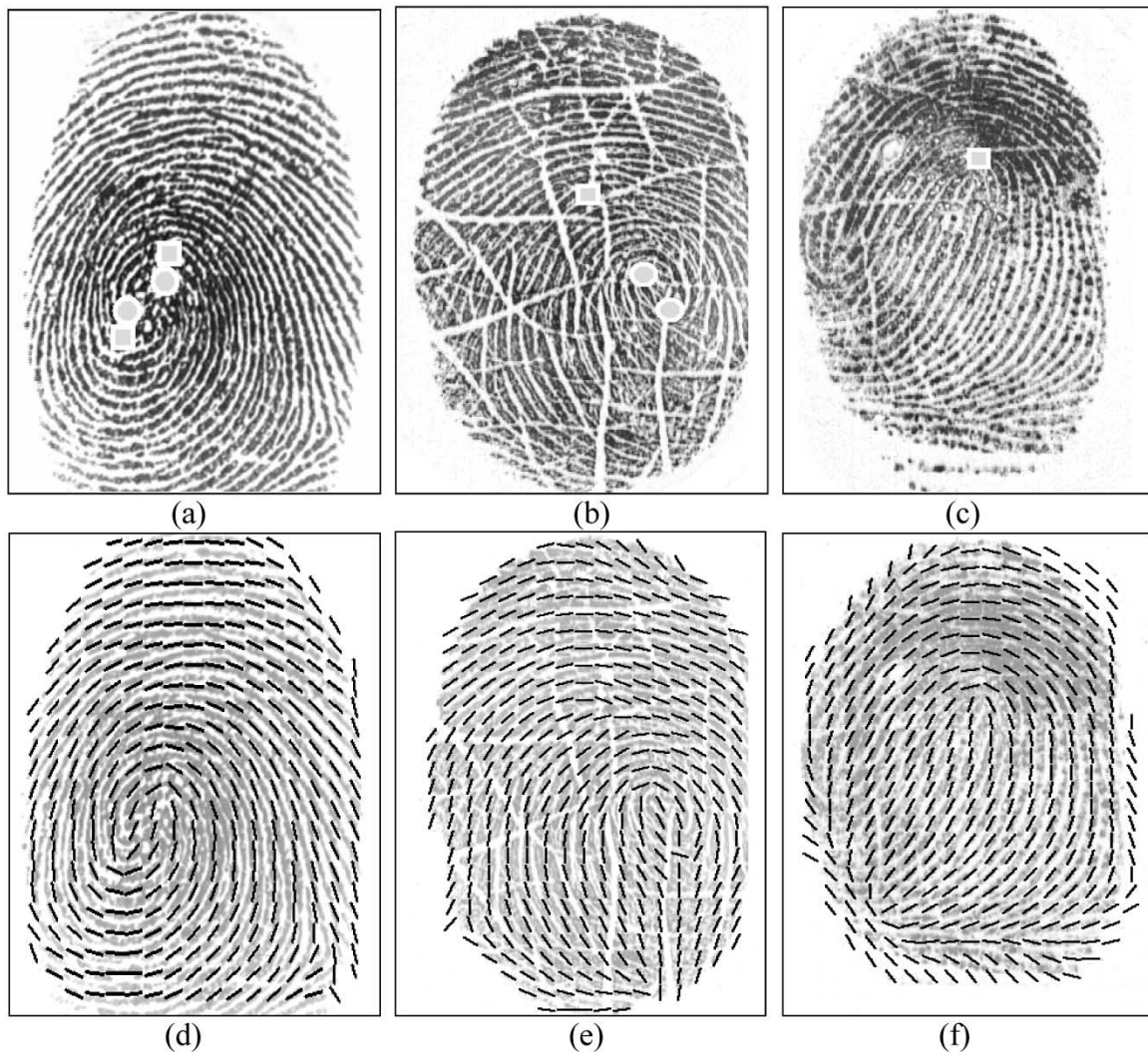


Fig. 12. Examples to illustrate the influence of unreliable singular points detection: (a) is a fingerprint image with two displaced core points, in which the true core points and the displaced cores are marked with circles and squares, respectively; (b) is a fingerprint image with a false core point, which is marked with a square; (c) is a with a missing core point in the middle-left part; and (d), (e), and (f) are their corresponding orientation fields detected by the model-based method respectively.

happen more frequently. In 480 images used in our experiments, false or missing singular points are detected in less than 3% of all images, and displaced singular points, whose distance from the detected positions to real positions are larger than twice the ridge's width (about 16 pixels), happen in less than 8% of the images.

Due to global approximation, the displaced, false or missing singular points results in inaccuracy only in a very small neighborhood of them, and in most regions of the fingerprints, the orientation can still be estimated accurately and robustly. In Fig. 12, several examples of displaced, false and missing singular points are given, in which the original fingerprint images are listed in the first row, and their corresponding orientation fields detected by the model-based algorithm are listed in the second row. (a) and (d) are for a fingerprint image with two displaced core points, in which the true core points and the displaced cores are marked with circles and squares, respectively; (b) and (e) are for a fingerprint image with a false core point, which is marked with a square; (c) and (f) are for a missing core point in the middle-left part. From each result, we can see

that only a small part of orientation field is affected by the displaced, false or missing singular points, and in most regions, the model-based algorithm performs rather satisfactorily.

B. Application Evaluation

Since the estimation of orientation field is a basic step for a fingerprint recognition system, the performance of the system can also reflect the performances of the orientation field estimation method. We have implemented a fingerprint recognition system using the model-based orientation estimation algorithm and compared it with applying the hierarchical gradient-based method on the THU database of our own lab (we did not test the filter-bank-based method because of its heavy computational cost).

The THU database is quite similar with the databases used in [6], [7]. It contains a total 1760 fingerprint images, i.e. 8 fingerprints (sized 512×320) per finger from 220 individuals, which were captured with live-scanners manufactured by Digital Persona Inc.. There were no restrictions of the impression's position and direction when these fingerprints were captured. These

fingerprint images varied with different qualities. About 75% of them are of reasonable qualities, and the remaining 25% are not of good qualities (similar with or worse than the images listed in Fig. 7).

The whole fingerprint recognition system consists of two parts, i.e., processing part and matching part, and the processing part mainly includes the steps of effective region segmentation, orientation field estimation, ridge enhancement, ridge thinning, and minutiae extraction (see Fig. 3). The important steps are briefly described as below.

A. Effective region segmentation

The fingerprint image is divided into many blocks (whose size is 16×16 pixels). For each block, the variance of the gray levels is computed. If the value exceeds the predefined threshold, this block is regarded as an effective block. Combining all effective blocks together, some post-process steps are taken, such as dilation and erosion in mathematical morphologic.

B. Orientation field estimation

In this step, the model-based orientation field estimation method and the hierarchical gradient-based method (in which the threshold of consistency level is chosen as $\pi/6$) are utilized, respectively.

C. Ridge enhancement

The method used here is quite similar with that used in [6], [7]. Since the gray-level values on ridges attain their local maxima along a direction normal to the local ridge orientation. Pixels can be identified to be ridge pixels based on this property. The fingerprint image is convolved with a matched Gabor-like filter, which is capable of adaptively accentuating the local maximum gray-level values along a direction normal to the local ridge orientation. Then a threshold can be easily chosen to segment the ridges adaptively.

D. Ridge thinning

The thinning technique proposed in [28] is utilized here.

E. Minutiae extraction

Operating on the thinned image, the minutiae are straightforward to detect: endings of the ridges are found at the termination of the lines and bifurcations are found at the junctions of three lines. But there will always be extraneous minutiae found due to a noisy image or artifacts introduced during the filtering and thinning. So some post-processing steps are needed to reduce the extraneous features: a bifurcation having a branch shorter than a defined threshold is eliminated; two endings of a short line are eliminated; two endings that are closely opposing each other are eliminated; endings at the boundary of the effective region are also eliminated. Then the following parameters are recorded for each surviving minutiae: (1) x -coordinate, (2) y -coordinate, and (3) local ridge orientation.

F. Minutiae matching

First a Hough transform is used to convert point pattern matching to a problem of detecting the highest peaks in the Hough space of transformation parameters. It accumulates evidence in the discretized space

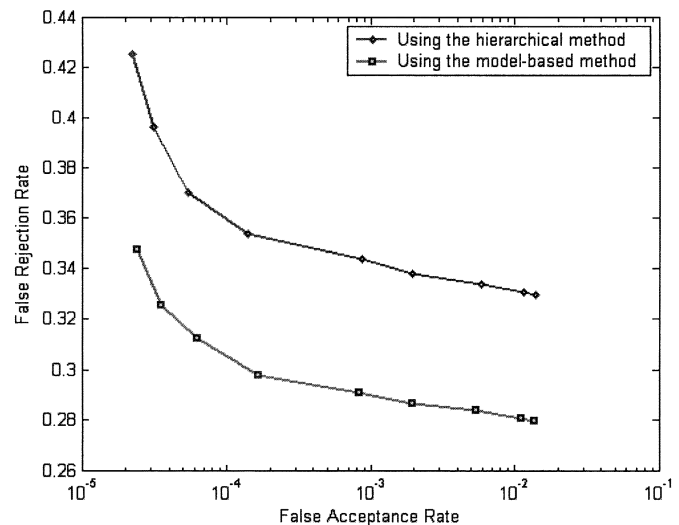


Fig. 13. ROC curves of two fingerprint-recognition systems by using the model-based orientation field estimation method and the hierarchical gradient-based method [6], [7], respectively.

of the transformation parameter by deriving transformation parameters that relate each two points from the input minutiae and the template minutiae [29]. The transformation parameters corresponding to the highest peak will be used for the registration. Then translate and rotate the input minutiae according to the registration parameters. By comparing these two sets of minutiae, a matching can be achieved by placing a bounding box around each point in the template minutiae and finding a point from the input minutiae in the box. The error between the matched pair is defined as the weighted sum of their distance and orientation's difference. Then, the matching score between the input fingerprint and the template fingerprint is computed by using the number of the matched pairs minus the averaged error of all matched pairs.

As to the two systems (i.e. using the model-based orientation field estimation method and the hierarchical gradient-based method), only the orientation estimation step are different and all the other steps are as the same. So, the performances of the two orientation field estimation methods can be fairly compared by the final recognition results of these two systems.

First, each fingerprint in the database is matched with the other fingerprints. A matching is labeled correct if these two fingerprints are of the same individual. A total of 3 095 840 (1760×1759) matchings have been performed, in which the number of true matchings should be 12 320 ($8 \times 7 \times 220$). The false rejection rate (FRR) and false acceptance rate (FAR) of two systems with different threshold values are recorded and their receiver operating curves (ROC) plotting FAR versus FRR are given in Fig. 13. The false rejection rate is defined as the percentage of true matchings (i.e. two fingerprints belonging to a same finger) with the matching score less than the threshold value. The false acceptance rate is defined as the percentage of wrong matchings (i.e. two fingerprints belonging to different fingers) with the matching score more than the threshold. From Fig. 13, we can see that FRR can be reduced more than 5% on average by

TABLE III

MATCHING RATES OF TWO FINGERPRINT RECOGNITION SYSTEMS BY USING THE MODEL-BASED ORIENTATION FIELD ESTIMATION METHOD AND THE HIERARCHICAL GRADIENT-BASED METHOD [6], [7], RESPECTIVELY, ON THE DATABASE USING THE LEAVE-ONE-OUT STRATEGY

Number of best matches	Matching Rate	
	Using the hierarchical method	Using the model-based method
1	0.979545	0.990341
2	0.970739	0.981250
3	0.956439	0.964962
4	0.936932	0.950852
5	0.908182	0.929545
6	0.872538	0.907008
7	0.831494	0.877029

using the model-based orientation field estimation method instead of the hierarchical gradient-based method. In Table III, the matching rates of these two systems (i.e. using the model-based method and the hierarchical gradient-based method) are also listed, which is defined as the percentage of correct fingerprints (of the same finger) present among the best n ($n = 1, \dots, 7$) matches. It shows that the matching rate can be improved from 0.8% to 4.5% (about 2% on average) by using the model-based method with different n .

V. CONCLUSIONS

In orientation field estimation algorithms, the filter-bank based approaches are more robust to noise than the gradient-based approaches, but they are inaccurate and computationally expensive. Contrastively, the gradient-based approaches lacks in robustness. In this paper, a model-based method for the computation of orientation field is proposed. First a combination model is established for the representation of the orientation field by considering its smoothness except for several singular points. When the coarse field is computed by using the gradient-based algorithm, the error from the noise can be eliminated using the model for a weighted approximation. Experimental results show that our algorithm has a better performance on robustness, accuracy and computational cost for orientation field estimation than the previous works. The application in a fingerprint recognition system also shows that an evident improvement can be obtained by using model-based orientation field estimation method.

Our further work is the application of this model for the match stage of fingerprint recognition. It is feasible to develop some novel algorithms for fingerprint recognition based on ridge orientation model, in which the coefficients of orientation model can be used for fingerprint matching.

ACKNOWLEDGMENT

The authors wish to acknowledge support from Natural Science Foundation of China, Natural Science Foundation of Beijing, National 863 Hi-Tech Development Program of China, and Basic Research Foundation of Tsinghua University. They would also like to thank anonymous reviewers for their valuable comments.

REFERENCES

- [1] A. K. Jain, R. Bolle, and S. Pankanti, Eds., *BIOMETRICS: Personal Identification in Networked Society*. New York: Kluwer, 1999.
- [2] D. Zhang, *Automated Biometrics: Technologies and Systems*. New York: Kluwer, 2000.
- [3] K. Hrechak and J. A. McHugh, "Automated fingerprint recognition using structural matching," *Pattern Recognit.*, vol. 23, pp. 893–904, 1990.
- [4] R. S. Germain, A. Califano, and S. Colville, "Fingerprint matching using transformation parameter clustering," *IEEE Comput. Science Eng.*, vol. 4, no. 4, pp. 42–49, 1997.
- [5] S. Pankanti, S. Prabhakar, and A. K. Jain, "On the individuality of fingerprints," *IEEE Trans. Pattern Anal. Machine Intell.*, vol. 24, no. 8, pp. 1010–1025, 2002.
- [6] A. Jain and L. Hong, "On-line fingerprint verification," *IEEE Trans. Pattern Anal. Machine Intell.*, vol. 19, no. 4, pp. 302–314, 1997.
- [7] A. Jain, L. Hong, S. Pankanti, and R. Bolle, "Identity authentication using fingerprints," *Proc. IEEE*, vol. 85, no. 9, pp. 1365–1388, 1997.
- [8] A. M. Bazen and S. H. Gerez, "Systematic methods for the computation of the directional fields and singular points of fingerprints," *IEEE Trans. Pattern Anal. Machine Intell.*, vol. 24, no. 7, pp. 905–919, 2002.
- [9] A. K. Jain, S. Prabhakar, and L. Hong *et al.*, "Filterbank-based fingerprint matching," *IEEE Trans. Image Processing*, vol. 9, no. 5, pp. 846–859, 2000.
- [10] A. Jain, S. Prabhakar, and L. Hong, "A multichannel approach to fingerprint classification," *IEEE Trans. Pattern Anal. Machine Intell.*, vol. 21, no. 4, pp. 348–359, 1999.
- [11] K. Karu and A. K. Jain, "Fingerprint classification," *Pattern Recognit.*, vol. 17, no. 3, pp. 389–404, 1996.
- [12] L. O'gorman and J. V. Nickerson, "An approach to fingerprint filter design," *Pattern Recognit.*, vol. 22, no. 1, pp. 29–38, 1989.
- [13] C. L. Wilson, G. T. Candela, and C. I. Watson, "Neural network fingerprint classification," *J. Artif. Neural Network*, vol. 1, no. 2, pp. 203–228, 1994.
- [14] M. Kawagoe and A. Tojo, "Fingerprint pattern classification," *Pattern Recognit.*, vol. 17, no. 3, pp. 295–303, 1984.
- [15] P. Perona, "Orientation diffusions," *IEEE Trans. Image Processing*, vol. 7, no. 3, pp. 457–467, 1998.
- [16] B. Sherlock and D. Monro, "A model for interpreting fingerprint topology," *Pattern Recognit.*, vol. 26, no. 7, pp. 1047–1055, 1993.
- [17] P. Vizcaya and L. Gerhardt, "A nonlinear orientation model for global description of fingerprints," *Pattern Recognit.*, vol. 29, no. 7, pp. 1221–1231, 1996.
- [18] E. R. Henry, *Classification and Uses of Finger Prints*. London, U.K.: Routledge, 1900.
- [19] N. I. Fisher, *Statistical Analysis of Circular Data*. Cambridge, U.K.: Cambridge Univ. Press, 1993.
- [20] G. H. Granlund and H. Knutsson, *Signal Processing for Computer Vision*. Norwell, MA: Kluwer, 1995.
- [21] M. Kass and A. Witkin, "Analyzing oriented pattern," *Comput. Vis., Graph., Image Process.*, vol. 37, pp. 362–397, 1987.
- [22] A. R. Rao, *A Taxonomy for Texture Description and Identification*. New York: Springer-Verlag, 1990.
- [23] J. Zhou, X. Lu, D. Zhang, and C. Y. Wu, "Orientation Analysis for Rotated Human Face Detection," *Image Vis. Comput.*, vol. 20, pp. 257–264, 2002.
- [24] J. Zhou, L. Xin, and D. Zhang, "Scale-orientation histogram for texture image retrieval," *Pattern Recognit.*, vol. 36, no. 4, pp. 1061–1063, 2003.
- [25] P. Whittle, *Prediction and Regulation by Linear Least-Square Methods*. London, U.K.: The English Universities Press Ltd, 1963.
- [26] NIST Special Database 14: NIST Mated Fingerprint Card Pairs (MFPC2) <http://www.nist.gov/srd/nistsd14.htm> [Online]
- [27] D. Maio, D. Maltoni, R. Cappelli, J. L. Wayman, and A. K. Jain, "FVC2000: Fingerprint verification competition," *IEEE Trans. Pattern Anal. Machine Intell.*, vol. 24, no. 3, pp. 402–412, 2002.
- [28] S. Zhang and K. S. Fu, "A thinning algorithm for discrete binary image," in *Proc. Int. Conf. Computers and Applications*, Beijing, China, 1984, pp. 879–886.
- [29] G. Stockman, S. Kopstein, and S. Benett, "Matching images to models for registration and object detection via clustering," *IEEE Trans. Pattern Anal. Machine Intell.*, vol. 4, no. 3, pp. 229–241, 1982.



Jie Zhou (M'01) was born in November 1968. He received the B.S. and M.S. degrees from Department of Mathematics, Nankai University, Tianjin, China, in 1990 and 1992, respectively. He received the Ph.D. degree from the Institute of Pattern Recognition and Artificial Intelligence, Huazhong University of Science and Technology (HUST), Wuhan, China, in 1995.

From 1995 to 1997, he served as a postdoctoral fellow in Department of Automation, Tsinghua University, Beijing, China. He is now Professor and As-

stant Director in Department of Automation, Tsinghua University. His research area includes pattern recognition, information fusion, image processing, and computer vision. He has directed or participated more than ten important projects. In recent years, he has published more than ten technical papers in international journals and more than 30 papers in international conferences.

Dr. Zhou is a fellow of Chinese Association of Artificial Intelligence (CAAI). He received the Best Doctoral Thesis Award from HUST and First Class Science and Technology Progress Award from the Ministry of Education, China, in 1995 and 1998, respectively.



Jinwei Gu was born in August 1980. He received the B.S. degree from Department of Automation, Tsinghua University, Beijing, China, in 2002. Now he is a masters student in Department of Automation, Tsinghua University.

His research interests are in pattern recognition, computer vision and intelligent information processing. He has published three papers in international journals and two papers in international conferences.